

Showcasing research from the Bengang Xing laboratory in the Division of Chemistry and Biological Chemistry, School of Physical and Mathematical Sciences at Nanyang University, Singapore.

**Title:** Metallic nanoparticles bioassay for *Enterobacter cloacae* P99  $\beta$ -lactamase activity and inhibitor screening

Gold and silver nanoparticles were employed in a colorimetric assay for bacterial enzyme detection and inhibitor screening. Taking advantage of the extent of nanoparticles aggregation following by distinct color change, this simple and specific colorimetric assay may offer a new way to study the inhibition of bacterial drug resistance.

As featured in:



Bengang Xing *et al.*,  
*Analyst*, 2010, **135**, 1031–1036

RSC Publishing

[www.rsc.org/analyst](http://www.rsc.org/analyst)

Registered Charity Number 207890

# Metallic nanoparticles bioassay for *Enterobacter cloacae* P99 $\beta$ -lactamase activity and inhibitor screening†

Rongrong Liu,<sup>a</sup> Weiling Teo,<sup>a</sup> Siyu Tan,<sup>a</sup> Huajun Feng,<sup>a</sup> Parasuraman Padmanabhan<sup>b</sup> and Bengang Xing<sup>\*a</sup>

Received 21st December 2009, Accepted 3rd February 2010

First published as an Advance Article on the web 19th February 2010

DOI: 10.1039/b926909f

This article presents a simple colorimetric assay for *Enterobacter cloacae* P99  $\beta$ -lactamase activity detection and its inhibitors screening on the basis of silver and gold nanoparticles aggregation. In the presence of *E. cloacae* P99  $\beta$ -lactamase, the  $\beta$ -lactam ring in the cephalosporin substrate was opened and resulted in releasing the active sites-modified linker which induced significant aggregation of silver or gold nanoparticles based on the electrostatic interactions and metal-thiols conjugation between the flexible linker and citrates on the surfaces of silver and gold nanoparticles. This aggregation process was associated with a concomitant color change of the nanoparticles solution and a red-shift of the particle surface plasmon resonance band, which was monitored by the naked eye or UV-Vis spectrophotometry. With this simple and convenient colorimetric assay, the activity of *E. cloacae* P99  $\beta$ -lactamase with a concentration as low as 16 pM could be easily visualized on the basis of gold nanoparticles aggregation. Silver nanoparticles provide a more sensitive assay toward the *E. cloacae* P99  $\beta$ -lactamase by which the lowest enzyme concentration down to 5.0 pM could be determined. Moreover, this effective colorimetric assay was also found useful for quantitative screening of *E. cloacae* P99  $\beta$ -lactamase inhibitors. Both the silver and gold nanoparticles exhibited identical trends for the *E. cloacae* P99  $\beta$ -lactamase inhibition screening, which were consistent with the results as determined by the standard assay. The results clearly indicated that the silver and gold nanoparticle based colorimetric assay may offer a new way to accurately evaluate the effect on the inhibition of bacterial drug resistance. Furthermore, the quantitative measurements presented in this work may also open the way for other relevant applications in prodrug development for cancer treatment.

## Introduction

$\beta$ -Lactamases (Blas) are a family of bacterial enzymes which could efficiently and irreversibly cleave the amide bond of  $\beta$ -lactam ring, and make  $\beta$ -lactam antibiotics ineffective toward the bacterial infection.<sup>1</sup> Usually,  $\beta$ -lactamases have been classified into four classes A, B, C and D on the basis of their molecular structures and substrate spectrum. Classes A, C and D possess a catalytic serine hydroxyl group as nucleophilic agent which hydrolyzes the  $\beta$ -lactam ring efficiently, while the class B is metal-dependent  $\beta$ -lactamases containing zinc at the active site.<sup>2</sup> Among the different members in Bla family, classes A and C  $\beta$ -lactamases are the most clinically important enzymes responsible for the antibiotics resistance in bacteria. Class A Blas have been the most thoroughly studied for combating the increased antibiotic resistance in clinical therapy and for imaging the gene expression *in vitro*, in living cells and even animals.<sup>3–7</sup> In comparison with the well-exploited class A Blas counterparts,

class C enzymes are relatively less characterized. Although the geometries of the active sites in class C  $\beta$ -lactamases are similar to those in class A enzymes, there are significant differences between the size and arrangements of secondary structure elements in these two different classes of bacterial enzymes. Moreover, besides their important roles in antimicrobial drug resistance in clinic, class C Blas have also been recently reported as an efficient antibody directed enzyme prodrug therapy (ADEPT) platform in cancer research to maximize the concentration of the cytotoxic agent at the tumor,<sup>8</sup> by which one class C *Enterobacter cloacae* P99 Bla and tumor antibody conjugates react with cephalosporin prodrugs which localize on the targeted tumor cell surface. Cleavage of cephalosporin  $\beta$ -lactam ring could trigger the controlled release of antitumor agents previously attached to the 3' position of cephalosporin, resulting in tumor selective drug delivery. In terms of these important bi-functional properties, the development of a simple and reliable bioassay to efficiently identify class C  $\beta$ -lactamase activity and to screen their inhibitors will be clinically significant to combat bacterial resistance and improve the efficacy for the prodrug release in cancer therapy.

Within the past decade, nanosize metal particles have received a great deal of attention in nanobiotechnology due to their novel optical and electronic properties.<sup>9</sup> Normally, the noble metals exhibit the strong surface plasmon resonance which allows them to present the intense color in the colloidal solution. The exact surface plasmon absorption is dependent on several parameters

<sup>a</sup>Division of Chemistry and Biological Chemistry, School of Physical and Mathematical Sciences, Nanyang Technological University, Singapore 637371. E-mail: Bengang@ntu.edu.sg; Tel: +65-63168758

<sup>b</sup>Translational Molecular Imaging Group (TMIG), Singapore, Bio-Imaging Consortium (SBIC), A\*Star, Singapore 138667

† Electronic supplementary information (ESI) available: Colorimetric assays toward *E. cloacae* P99 Bla activity and inhibition by nitrocefin and analysis of *E. cloacae* P99 Bla purity by SDS-PAGE. See DOI: 10.1039/b926909f

such as shape, size, medium, the distance between particles or the type of metals.<sup>10</sup> For example, the dispersed gold nanoparticles (AuNPs) around 16 nm diameter have a red color with a surface plasmon absorption band centered at 520 nm. When the interparticle distance decreases to less than the diameter of the particle, the coupling interactions result in a red-shift of the resonance wavelength and also lead to significant aggregation of AuNPs with the distinctive color change from red to blue. Similarly, the monodispersed silver nanoparticles (AgNPs) in solution are a yellow color with the size dependent surface plasmon resonance between ~390 and 420 nm. Upon aggregation, the silver nanoparticles appear an orange-red color with the resonance band shifting to a longer wavelength. The color change associated with nanoparticles aggregation possesses high extinction coefficients which are usually over one thousand times larger than those of traditional organic chromophores.<sup>11</sup> Therefore, both the silver and gold nanoparticles have been extensively exploited in the development of colorimetric assay for the detection of nucleic acids,<sup>11,12a-c</sup> proteins,<sup>12d-g</sup> metal ions,<sup>12g-l</sup> and small molecules<sup>12m</sup> etc. Similar analytical methods have also been described as efficient tools for the control of the formation of nanoparticle assemblies, identification of enzyme activities or screening of their inhibitors.<sup>13</sup> In this study, we report a practical and easily operated colorimetric aggregation method by taking advantage of the significant color change and red-shift of plasmon resonance bands of gold and silver nanoparticles for the systematic determination of class C *E. cloacae* P99  $\beta$ -lactamase activity and screening of its inhibitors. Scheme 1 outlines the general principle and molecular design of this assay. The short polyethylene glycol (PEG) modified 2-(4-mercaptophenyl) acetic acid was attached to the 3' position of cephalosporin, which is well known as a good substrate for class C *E. cloacae* P99  $\beta$ -lactamase.<sup>8</sup> Upon the action of enzyme hydrolysis, the  $\beta$ -lactam ring in the cephalosporin derivative is opened and leads to the release of the fragment containing the free thiol and

positively charged amino group, which substitutes the citrate ions on the surface of silver and gold nanoparticles and thereby results in the aggregation of these metallic nanoparticles due to the electrostatic interactions and silver or gold-thiols interactions. The aggregated silver and gold nanoparticles demonstrate the obvious color change and red-shift of their plasmon absorption bands. Exploiting the significant color change from silver or gold nanoparticles, it is possible to construct a simple and effective colorimetric assay for efficient detection of class C *E. cloacae* P99  $\beta$ -lactamase activity and screening of its inhibitors by either naked eye or simple UV-Vis absorbance measurement.

## Experimental

### Materials

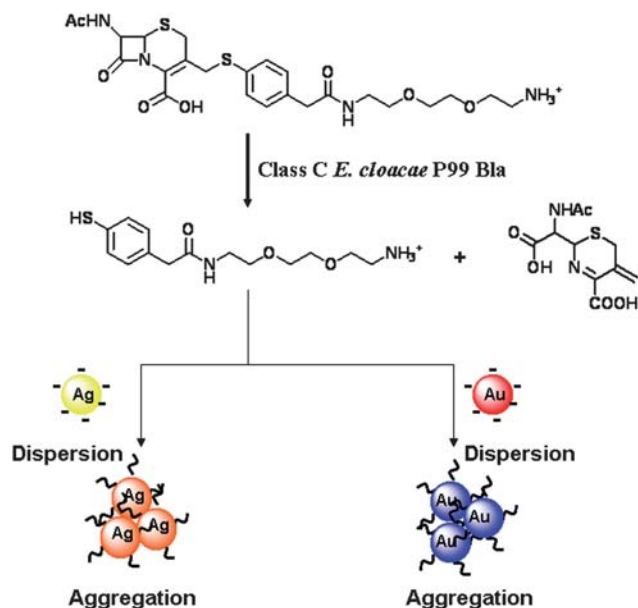
7-Amino-3-chloromethyl 3-cephem-4-carboxylic acid diphenylmethyl ester hydrochloride (ACLH) was provided from Otsuka chemical Co. Ltd. Nitrocefin was purchased from Merck. The purified class C *Enterobacter cloacae* P99  $\beta$ -lactamase was obtained from Sigma-Aldrich. The purity and isoform components of enzyme were analyzed by sodium dodecyl sulfate-polyacrylamide gel electrophoresis (SDS-PAGE) (see ESI†). All the other starting materials were obtained from Sigma or Aldrich. Commercially available reagents were used without further purification, unless noted otherwise. All other chemicals were analytical grade or better. The cephalosporin derivative was prepared as reported previously.<sup>13g</sup> The synthesized product was purified by reverse-phase HPLC (Shimadzu LC-20A) and characterized by using <sup>1</sup>H NMR (Bruker Advance 400MHz). ESI-MS spectrometric analysis was performed on the Thermo Finnigan LCQ Deca XP Max.

### Preparation of silver and gold nanoparticles

Silver nanoparticles (AgNPs) around 16 nm were prepared by chemical reduction of silver nitrate in sodium borohydride according to the reported method.<sup>14</sup> Briefly, silver nitrate (250  $\mu$ l of 100 mM) and sodium citrate (250  $\mu$ l of 100 mM) were added into 100 mL water followed by the addition of fresh NaBH<sub>4</sub> solution (5 mM, 6 mL) under vigorous stirring. The mixed solution was stirred for an additional 30 min and was left overnight before using. The pH of the vivid yellow colloid solution was adjusted to 7.4.

The 16 nm citrate-capped gold nanoparticles (AuNPs) were prepared by reduction of hydrogen tetrachloroaurate (HAuCl<sub>4</sub>).<sup>15</sup> The aqueous solution of HAuCl<sub>4</sub> (1 mM in 95 mL of deionized water) was refluxed for 20 min and followed by addition of 3 mL of 1% sodium citrate solution. The mixture was heated under reflux for another 30 min until the color of the solution change to wine-red. After cooling down to room temperature, the pH was adjusted to 7.4 and filtered through 0.45  $\mu$ m Millipore syringe to remove the precipitate; the filtrate was stored at room temperature.

Transmission Electron Microscope (TEM, JEOL 2000 EX, 120 kV) was used to provide the images of the as-synthesized silver and gold nanoparticles. The concentrations of AgNPs and AuNPs were determined by surface plasmon resonance absorbance at 400 nm and 520 nm, respectively.<sup>11a</sup> Absorbance spectra



**Scheme 1** Illustration of class C *E. cloacae* P99  $\beta$ -lactamase induced aggregation of AgNPs/AuNPs.

were measured on Beckman Coulter DU 800 UV-Vis spectrophotometer.

### Colorimetric assay for class C *E. cloacae* P99 Bla activity with silver and gold nanoparticles

In a typical experiment,  $\beta$ -lactam substrate was initially incubated with class C *E. cloacae* P99 Bla in phosphate buffered saline (PBS buffer, 10 mM, pH 7.4) at room temperature for 20 min. Then the mixed solution was transferred into the dispersed Ag or Au nanoparticles solution to afford 5.0  $\mu$ M of substrate and 3.0 nM of *E. cloacae* P99 Bla. The color change and UV-Vis absorbance were monitored as a function of time. Ag or Au nanoparticles solution containing intact substrate without enzyme treatment was used as control.

### Colorimetric assay for class C *E. cloacae* P99 Bla inhibition with silver and gold nanoparticles

Typically, class C *E. cloacae* P99 Bla was initially incubated with different inhibitors in phosphate buffered saline (PBS buffer, pH 7.4) for 10 min at room temperature to inhibit the enzyme activity. The cephalosporin based  $\beta$ -lactam substrate was subsequently added into the inhibitor-treated enzyme solutions for an additional 20 min incubation. Then, the aliquot of the above mixed solution was immediately transferred into the dispersed nanoparticles solution affording 5.0  $\mu$ M of substrate and 3.0 nM of class C *E. cloacae* P99 Bla. The color change and UV-Vis absorption spectra of AgNPs or AuNPs suspension were collected every two minutes for 30 min at 25  $^{\circ}$ C by Beckman Coulter DU 800 UV-Vis spectrophotometer. The quantitative  $IC_{50}$  measurements were conducted on the basis of absorbance change of nanoparticles at 5 min time point upon the addition of reaction mixtures into nanoparticles solutions. The control experiments indicated that substrate, class C *E. cloacae* P99  $\beta$ -lactamase and inhibitors would not induce the aggregation of AgNPs and AuNPs.

## Results and discussion

Hydrolysis of the  $\beta$ -lactam ring in cephalosporin derivative induces spontaneous elimination of any leaving groups attached to the 3'-position. In a typical experiment, the  $\beta$ -lactam substrate was initially incubated with class C *E. cloacae* P99 Bla in PBS buffer (pH 7.4). The aliquot of solution was then transferred into the dispersed AgNPs solution. As shown in Fig. 1A, the remarkable color change from vivid yellow to orange-red was found within seconds. The color change of AgNPs was also accompanied by the red-shift of surface plasmon resonance (SPR) peak from 400 nm to 550 nm upon the addition of the enzyme treated substrate into AgNPs solutions (Fig. 1A). As a control, the initial AgNPs solutions containing intact cephalosporin substrate were vivid yellow in color, demonstrating that the AgNPs solution were stable and the observed color change and spectrum shift were from the enzymatic interaction induced silver nanoparticles aggregation. Similar results were also found in the assay based on gold nanoparticles with the size of 16 nm. The AuNPs solution showed a red color with a typical plasmon absorption band around 520 nm, and addition of intact  $\beta$ -lactam substrate to the solution of AuNPs did not induce color change

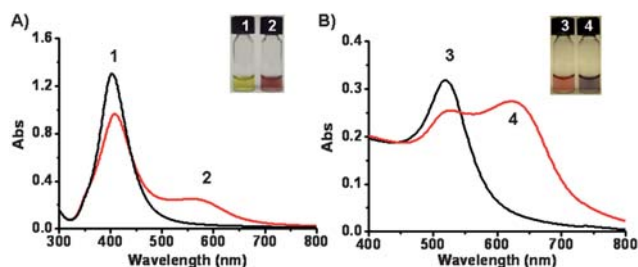


**Fig. 1** (A) UV-Vis absorption spectra of AgNPs before (black line) and after addition (red line) of *E. cloacae* P99 Bla (3.0 nM) treated substrate (5.0  $\mu$ M). The inset shows the color change of AgNPs. (1) AgNPs with substrate only and (2) AgNPs with Bla treated substrate. (B) UV-Vis absorption spectra of AuNPs before (black line) and after addition (red line) of class C *E. cloacae* P99 Bla treated substrate. The inset shows the color change of AuNPs. (3) AuNPs with substrate only and (4) AuNPs with Bla treated substrate.

and absorption spectral shifts. However, the obvious color change from red to blue was observed upon addition of *E. cloacae* P99 Bla treated substrate into AuNPs solution as shown in Fig. 1B. Both a decreased absorbance at 520 nm and an increased absorbance at 620 nm were observed in the UV-Vis spectrum with a prolonging of the reaction time.

The observed color change and spectral shifts from AgNPs and AuNPs aggregation provided a platform for quantitatively monitoring the process of class C *E. cloacae* P99 Bla enzymatic hydrolysis. Fig. 2 showed the quantitative relationship between the absorbance change and the concentration of *E. cloacae* P99 Bla for both silver and gold nanoparticles. The apparent color change and spectral shifts indicated that both silver and gold nanoparticles could be used for visualization of the enzymatic activity. The significant absorbance intensity enhancement from the dispersion to the full aggregation was observed in 2.5 nM of silver nanoparticle solutions with a near-linear correlation between the absorbance and the enzyme concentration in the range of 0–0.1 nM. This condition provided an effective colorimetric assay for *E. cloacae* P99 Bla detection with a good sensitivity as low as 5.0 pM with the dynamic range from 5.0 pM to 600 pM.<sup>13k</sup> As for similar assay based on gold nanoparticles (Fig. 2B), the overall color change and absorbance intensity enhancement in the linear range of 0.015–0.08 nM class C *E.*

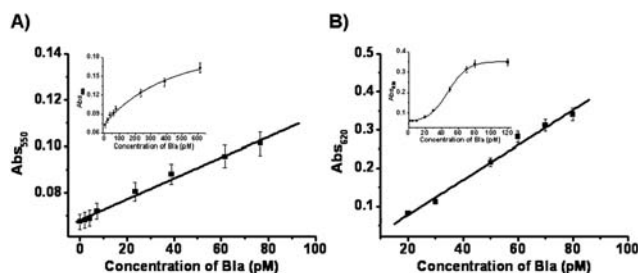


**Fig. 2** (A) Absorbance change at 550 nm of AgNPs at 2.5 nM with substrate (5.0  $\mu$ M) and varying the concentrations of class C *E. cloacae* P99 Bla. (B) Absorbance change at 620 nm of AuNPs at 2.5 nM with substrate (5.0  $\mu$ M) and varying the concentrations of class C *E. cloacae* P99 Bla. The inset indicates the observed absorbance change with higher concentration of enzyme.

*cloacae* P99 Bla enabled the effective enzyme detection with the lowest concentration down to 16 pM. The dynamic range of AuNPs assay was determined to range from 16 pM to 90 pM. Compared to the colorimetric assay based on AuNPs, AgNPs were more sensitive due to their higher extinction coefficient relative to the AuNPs with the same size.<sup>11b,14</sup>

The observed color change and absorption spectral shifts caused by the aggregation of silver or gold nanoparticles were confirmed by transmission electron microscope (TEM) analysis. As shown in Fig. 3, in the absence of *E. cloacae* P99 Bla, both the silver and gold nanoparticles were well dispersed and the cephalosporin derivative itself or enzyme inhibitors were unable to induce the aggregation of silver or gold nanoparticles (Fig. 3a, d). However, upon treatment with *E. cloacae* P99 Bla, cleavage of the  $\beta$ -lactam ring in cephalosporin induced the release of the free thiol and positively charged amino group contained flexible linker which induced the significant aggregation of silver and gold nanoparticles (Fig. 3b, e), thus demonstrating the distinctive color changes in the AgNPs and AuNPs solutions. As expected, in the presence of sufficient amount of efficient *E. cloacae* P99 Bla inhibitor such as aztreonam (ATM), the enzymatic activity would be dramatically suppressed and there was no significant nanoparticle aggregation observed. Therefore, the TEM results were very similar to those of AgNPs and AuNPs solutions without enzyme treatment (Fig. 3c, f). These results clearly demonstrated that the enzyme interactions between the cephalosporin derivative and class C *E. cloacae* P99 Bla played an important role in the aggregation of silver and gold nanoparticles. Upon treatment with effective enzyme inhibitors, both the AgNPs and AuNPs aggregation would be significantly decreased.

This easily operated colorimetric bioassay was also utilized in *E. cloacae* P99 Bla inhibitor screening. In the typical screening experiment,  $\beta$ -lactam substrate (5.0  $\mu$ M) was first incubated with *E. cloacae* P99 Bla (3.0 nM) in PBS buffer (pH 7.4) in the presence of one of the following  $\beta$ -lactamase inhibitors (0.3  $\mu$ M): aztreonam (ATM), clavulanate acid (CA), tazobactam (TZB),

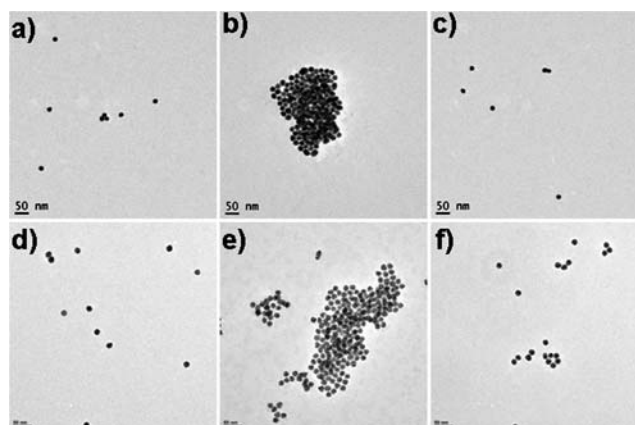


**Fig. 3** TEM images of AgNPs and AuNPs. (a) substrate (5.0  $\mu$ M) in AgNPs; (b) substrate (5.0  $\mu$ M) with *E. cloacae* P99 Bla in the absence and (c) presence of inhibitor aztreonam (1.0  $\mu$ M) in AgNPs solutions. (d) substrate (5.0  $\mu$ M) in AuNPs; (e) substrate (5.0  $\mu$ M) with *E. cloacae* P99 Bla in the absence and (f) presence of inhibitor aztreonam (1.0  $\mu$ M) in AuNPs solutions. Scale bar is 50 nm.

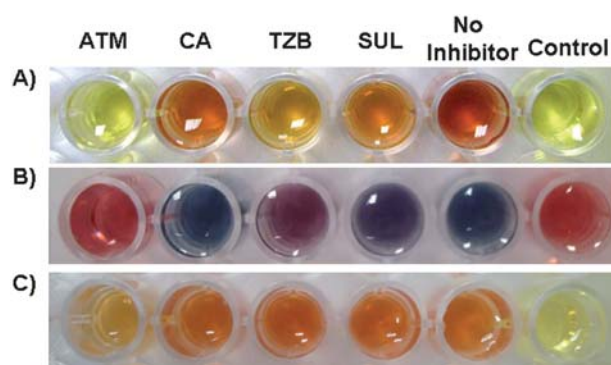


**Fig. 4** Colorimetric assay for *E. cloacae* P99 Bla inhibition in 96-well microplate with four different inhibitors. (A) AgNPs based assay with 0.3  $\mu$ M inhibitors; (B) AuNPs based assay with 0.3  $\mu$ M inhibitors; (C) Nitrocefin assay with 0.3  $\mu$ M inhibitors.

and sulbactam (SUL). Most of them are well known inhibitors that efficiently suppress class C Bla activities in clinics.<sup>16</sup> The resulting solutions were then transferred into silver or gold nanoparticle suspensions. The absorbance spectral variation of silver or gold nanoparticles at 550 nm or 620 nm was monitored as a function of time, and the color change of the nanoparticle solutions were determined with the naked eye and simple UV-Vis absorbance measurements. In a silver nanoparticle based enzyme inhibition assay, a yellow solution revealed the potent enzyme inhibition and an orange-red color demonstrated the weak inhibition and aggregation of AgNPs occurred at this stage. As shown in Fig. 4A, the observed yellow color in ATM indicated the strongest Bla inhibition. The slight orange color in TZB revealed the weaker inhibition than ATM and the orange color in SUL exhibited a weaker enzyme inhibition than those in ATM and TZB but stronger than that in CA. Similarly, in a gold nanoparticle based enzyme inhibition assay, a red color implied a significant effectiveness in the enzyme inhibition against aggregation whereas a blue color indicated the least inhibition and allowed the enzymatic reaction to proceed, resulting in the aggregation of AuNPs (Fig. 4B). The different colors associated with the different extents of aggregation provided the following enzyme inhibition trend: ATM > TZB > SUL > CA as shown in Fig. 5A and 5B. The observed trend for class C *E. cloacae* P99 Bla inhibitions in AuNPs based assay was identical with that using AgNPs. Both of these data were in agreement with the result as determined by the standard indicator nitrocefin when

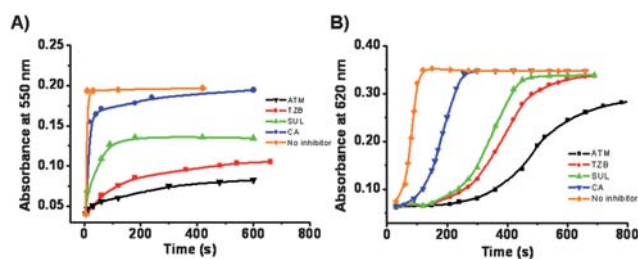


**Fig. 5** Time-course measurement of *E. cloacae* P99 Bla inhibition assay with AgNPs and AuNPs. (A) Substrate (5.0  $\mu$ M) and *E. cloacae* P99 Bla treated inhibitors (0.3  $\mu$ M) with AgNPs. (B) Substrate (5.0  $\mu$ M) and *E. cloacae* P99 Bla treated inhibitors (0.3  $\mu$ M) with AuNPs.

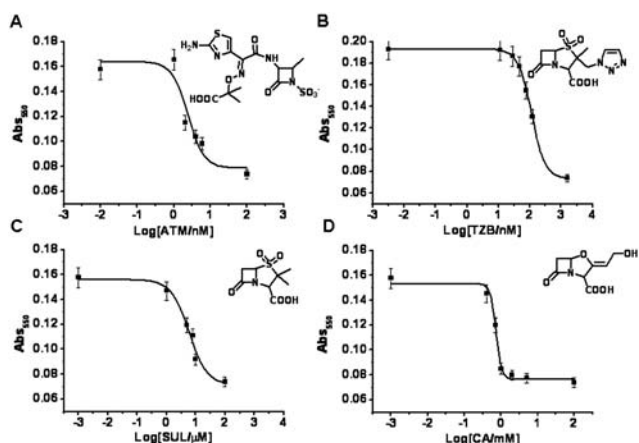


**Fig. 6** Inhibition assay of *E. cloacae* P99 Bla activity using ATM (A), TZB (B), SUL (C), and CA (D). The  $IC_{50}$  values were calculated from the absorbance change of AgNPs at 550 nm.

the higher inhibitor concentration was used in the enzyme inhibition assay (see ESI†). This result was also similar to the reported inhibitors binding affinities toward class C *E. cloacae* P99 Bla.<sup>16</sup> No significant color change among the different inhibitors could be observed in the nitrocefin assay under comparable conditions (Fig. 4C), demonstrating that both AgNPs and AuNPs based colorimetric inhibition assay exhibited more efficient properties to effectively screen the class C *E. cloacae* P99 Bla inhibitors.

In terms of the significant color change and absorption intensity enhancement in AgNPs and AuNPs, the effect of the enzyme inhibition was also quantitatively estimated by the colorimetric assay on the basis of AgNPs and AuNPs aggregation. As shown in Fig. 6, the corresponding  $IC_{50}$  values (concentration of inhibitor that reduces enzyme activity to 50% of the activity of the native enzyme) of the four inhibitors ATM, TZB, SUL and CA for *E. cloacae* P99 Bla were identified for AgNPs to be 0.0027, 0.157, 5.1 and 753  $\mu$ M respectively. Similarly, the  $IC_{50}$  values of these four inhibitors were also evaluated

to be 0.004, 0.144, 4.8 and 900  $\mu$ M based on the assay that used AuNPs (Fig. 7). These  $IC_{50}$  values were consistent with values obtained when nitrocefin was used (see ESI†) and were also comparable with values reported previously.<sup>16</sup> These results would suggest that metallic nanoparticles (such as silver or gold nanoparticles) based colorimetric bioassay could be used for the efficient identification of class C *E. cloacae* P99 Bla activity and high throughput screening of its inhibitors.

## Conclusions

In summary, a simple and practical colorimetric assay for class C *E. cloacae* P99  $\beta$ -lactamase activity and inhibitors screening has been successfully established with silver and gold nanoparticles and  $\beta$ -lactam cephalosporin substrate. Based on the hydrolysis of enzyme, the  $\beta$ -lactam ring in cephalosporin is cleaved and results in the release of the free thiol and positively charged amino containing linker which further induces the aggregation of silver or gold nanoparticles through the cross-linking interactions between the flexible linkers and the citrate ions on the surface of these metallic nanoparticles. The silver nanoparticles proved to provide an enzyme assay with higher sensitivity than that based on gold nanoparticles. Both metallic nanoparticles exhibit the unique feature for efficient screening of various enzyme inhibitors by the naked eye and simple UV-Vis absorbance measurements. These results clearly indicate that the metallic nanoparticle based colorimetric assay may offer a new way to study the efficacy for the effect on the inhibition of bacterial drug resistance. The quantitative measurements presented in this work may also open the way for other relevant applications in prodrug development for cancer treatment.

## Acknowledgements

This work was supported by start-up grant, SEP (RG139/06), A\*Star BMRC (07/1/22/19/534) and URC (RG56/06) grants in Nanyang Technological University.

## References

- C. T. Walsh, *Antibiotics: Actions, Origins and Resistance*, 1st ed., ASM Press: Washington, D.C., 2003.
- (a) J. F. Fisher, S. O. Meroueh and S. Mobashery, *Chem. Rev.*, 2005, **105**, 395–424; (b) J. Spencer and T. R. Walsh, *Angew. Chem. Int. Ed.*, 2006, **45**, 1022–1026; (c) K. Bush, *Antimicrob. Resist.*, 2001, **32**, 1085–1089; (d) E. Lobkovsky, E. M. Billings, P. C. Moews, J. Rahil, P. F. Pratt and J. R. Knox, *Biochemistry*, 1994, **33**, 6762–6772.
- S. N. Maiti, O. A. Philips, R. G. Micetich and D. M. Livermore, *Curr. Med. Chem.*, 1998, **5**, 441–456.
- V. P. Sandanayaka and A. S. Prasad, *Curr. Med. Chem.*, 2002, **9**, 1145–1165.
- G. Zlokarnik, P. A. Negulescu, T. E. Knapp, L. Mere, N. Burres, L. Feng, M. Whitney, K. Roemer and R. Y. Tsien, *Science*, 1998, **279**, 84–88.
- (a) W. Z. Gao, B. G. Xing, R. Y. Tsien and J. H. Rao, *J. Am. Chem. Soc.*, 2003, **125**, 11146–11147; (b) B. G. Xing, K. Ashot and J. H. Rao, *J. Am. Chem. Soc.*, 2005, **127**, 4158–4159; (c) H. Q. Yao, M. K. So and J. H. Rao, *Angew. Chem. Int. Ed.*, 2007, **46**, 7031–7033.
- M. Cavois, C. de Noronha and W. C. Greene, *Nat. Biotechnol.*, 2002, **20**, 1151–1154.
- (a) M. L. Rodrigues, P. Carter, C. Wirth, S. Mullins, A. Lee and B. K. Blackburn, *Chem. Biol.*, 1995, **2**, 223–227; (b) B. G. Xing, J. H. Rao and R. R. Liu, *Mini-Rev. Med. Chem.*, 2008, **8**, 455–471; (c) V. M. Vrudhula, H. P. Svensson and P. D. Senter, *J. Med. Chem.*, 1997, **40**, 2788–2792; (d) R. Satchi-Fainaro, H. Hailu,

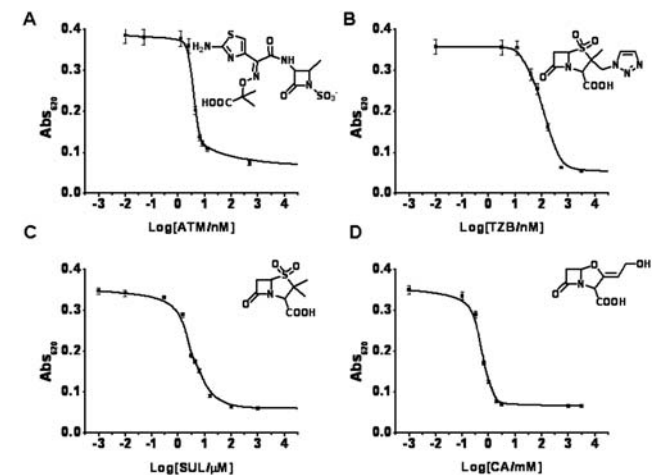


**Fig. 7** Inhibition assay of *E. cloacae* P99 Bla activity using ATM (A), TZB (B), SUL (C), and CA (D). The  $IC_{50}$  values were calculated from the absorbance change of AuNPs at 620 nm.

- J. W. Davies, C. Summerford and R. Duncan, *Bioconjugate Chem.*, 2003, **14**, 797–804.
- 9 D. A. Schultz, *Curr. Opin. Biotechnol.*, 2003, **14**, 13–22.
- 10 (a) B. Nikoobakht and M. A. El-Sayed, *Chem. Mater.*, 2003, **15**, 1957–1961; (b) K. H. Su, Q. H. Wei, X. Zhang, J. J. Mock, D. R. Smith and S. Schultz, *Nano Lett.*, 2003, **3**, 1087–1090; (c) Y. G. Sun and Y. N. Xia, *Science*, 2002, **298**, 2176–2179.
- 11 (a) R. Jin, G. Wu, Z. Li, C. A. Mirkin and G. C. Schatz, *J. Am. Chem. Soc.*, 2003, **125**, 1643–1654; (b) J. S. Lee, A. K. R. Lytton-Jean, S. J. Hurst and C. A. Mirkin, *Nano Lett.*, 2007, **7**, 2112–2115; (c) J. Ling, Y. Yang and C. Z. Huang, *J. Pharm. Biomed. Anal.*, 2004, **35**, 185–191; (d) C. D. Medley, J. E. Smith, Z. W. Tang, Y. R. Wu, S. Bamrungsap and W. H. Tan, *Anal. Chem.*, 2008, **80**, 1067.
- 12 (a) R. Elghanian, J. J. Storhoff, R. C. Mucic, R. L. Letsinger and C. A. Mirkin, *Science*, 1997, **277**, 1078–1081; (b) L. Li and L. Rothberg, *Proc. Natl. Acad. Sci. USA*, 2004, **101**, 14036–14039; (c) C. M. Niemeyer, *Angew. Chem. Int. Ed.*, 2001, **40**, 4128–4158; (d) B. Li, H. Wei and S. Dong, *Chem. Comm.*, 2007, 73–75; (e) S. P. Song, Z. Q. Liang, J. Zhang, L. H. Wang, G. X. Li and C. H. Fan, *Angew. Chem. Int. Ed.*, 2009, **48**, 8670; (f) C. L. Schofield, A. H. Haines, R. A. Field and D. A. Russell, *Langmuir*, 2006, **22**, 6707–6711; (g) Y. M. Chen, C. J. Yu, T. L. Cheng and W. L. Tseng, *Langmuir*, 2008, **24**, 3654–3660; (h) W. Liu, Y. Lu and J. Liu, *Acc. Chem. Res.*, 2007, **40**, 315; (i) J. W. Liu, Z. H. Cao and Y. Lu, *Chem. Rev.*, 2009, **109**, 1948; (j) Y. Zhou, S. X. Wang, K. Zhang and X. Y. Jiang, *Angew. Chem. Int. Ed.*, 2008, **47**, 7454–7456; (k) S. O. Obare, R. E. Hollowell and C. J. Murphy, *Langmuir*, 2002, **18**, 10407–10410; (l) C. Guarise, L. Pasquato and P. Scrimin, *Langmuir*, 2005, **21**, 5537–5541; (m) X. W. Xu, J. Wang, F. Yang, K. Jiao and X. R. Yang, *Small*, 2009, **5**, 2669–2672.
- 13 (a) Z. Wang, R. Levy, D. G. Fernig and M. Brust, *J. Am. Chem. Soc.*, 2006, **128**, 2214–2215; (b) C. Guarise, L. Pasquato, V. De Filippis and P. Scrimin, *Proc. Natl. Acad. Sci. USA*, 2006, **103**, 3978–3982; (c) A. Laromaine, L. Koh, M. Murugesan, R. V. Ulijn and M. M. Stevens, *J. Am. Chem. Soc.*, 2007, **129**, 4156–4157; (d) Y. D. Choi, N. H. Ho and C. H. Tung, *Angew. Chem. Int. Ed.*, 2007, **46**, 707–709; (e) R. R. Liu, R. Liew, J. Zhou and B. G. Xing, *Angew. Chem. Int. Ed.*, 2007, **46**, 8799–8803; (f) M. Wang, X. G. Gu, G. X. Zhang, D. Q. Zhang and D. B. Zhu, *Langmuir*, 2009, **25**, 2504–2507; (g) T. T. Jiang, R. R. Liu, X. F. Huang, H. J. Feng, W. L. Teo and B. G. Xing, *Chem. Comm.*, 2009, **15**, 1972; (h) X. Y. Xu, M. S. Han and C. A. Mirkin, *Angew. Chem. Int. Ed.*, 2007, **46**, 3468–3470; (i) V. Pavlov, Y. Xiao and I. Willner, *Nano Lett.*, 2005, **5**, 649–653; (j) J. Oishi, Y. Asami, T. Mori, J. H. Kang, M. Tanabe, T. Niidome and Y. Katayama, *Chembiochem*, 2007, **8**, 875–879; (k) Y. L. Wang, D. Li, W. Ren, Z. J. Liu, S. J. Dong and E. K. Wang, *Chem. Commun.*, 2008, **14**, 2520.
- 14 (a) H. Wei, C. G. Chen, B. Y. Han and E. K. Wang, *Anal. Chem.*, 2008, **80**, 7051–7055; (b) D. G. Thompson, A. Enright, K. Faulds, W. E. Smith and D. Graham, *Anal. Chem.*, 2008, **80**, 2805–2810; (c) R. Kanjanawarut and X. D. Su, *Anal. Chem.*, 2009, **81**, 6122–6129.
- 15 G. Frens, *Nature Physical Science*, 1973, **241**, 20–22.
- 16 (a) K. Bush, C. Macalintal, B. A. Rasmussen, V. J. Lee and Y. Yang, *Antimicrob. Agent Chemother.*, 1993, **37**, 851–858; (b) K. Bush, G. A. Jacoby and A. A. Medeiros, *Antimicrob. Agents Chemother.*, 1995, **39**, 1211–1233.